Experimental modeling of a web-winding machine: LPV approaches

Chapter 1

Experimental Modelling of a Web Winding Machine: LPV Approaches

Jose Vuelvas [1] Fredy Ruiz[2] and Carlo Novara [3]

This chapter presents the identification of a web winding system as an LPV system with the reel radius as the time-varying parameter. This system is non-linear, time-varying and input-output unstable. Two identification methods are considered: In the first one, an LPV model is estimated in a single step using a novel approach based on sparse identification and Set Membership optimality evaluation. In the second one, several local LTI models are identified using classical identification algorithms and the overall LPV model is constructed as a weighted sum of the local models. The two methods are applied to experimental data measured on a real web winding machine.

Keywords—LPV models; Web Winding System; Sparse Identification; Model interpolation.

1.1 Introduction

Web winding systems are very common in industry, for example, in the production of materials such as paper, cloth, plastic, wire, sheets and steel. In order to guarantee integrity and quality standards, automatic control systems are implemented to regulate the tension and speed of the material as it is transported from one reel to another, so that the process is run at the desired time, ensuring that the final product does not suffer deformations or breaks that may block the process line. One characteristic of these systems is their time-varying behavior, due to the accumulation of material that causes variations in the reel radius, resulting in changes in the moment of inertia of the motor load. That is, these systems have the reel radius as time-varying parameter.

Several approaches to modeling of web winding systems can be found in the literature. White-box models, based on first principles, are presented in [1–4]. These models are non-linear, time-varying and input-output unstable. Black-box approaches have also been proposed, based on different identification techniques. In [5] and [6], MIMO (multi-input multi-output) LTI (linear time-invariant) models are estimated

[1]Pontificia Universidad Javeriana, Bogotá,Colombia
[2]Pontificia Universidad Javeriana, Bogotá,Colombia
[3]Politecnico di Torino, Turin, Italy

by sub-spaces techniques. In [7] a set of MISO (multiple input single output) models are estimated by instrumental variables methods. Grey-box models, which are a combination of the two previous types, are developed in [8, 9], where the friction in each motor is estimated using least squares with data acquired with constant speed. The moment of inertia of the motors and the gain of the torques are identified using model fitting techniques.

Due to the nonlinear and time-varying nature of the web winding system, linear time-invariant control systems do not give in general adequate performances in terms of disturbance rejection, while gain-scheduling controllers are expected to provide high performances, since these controllers can effectively deal with nonlinearities and time-varying parameters. This motivates the need of accurate LPV (linear parameter-varying) models of the web winding system, which may allow the design of efficient gain-scheduling controllers. Note that, because of the intrinsic system instability, model identification and validation are quite challenging tasks.

In the literature, several LPV identification techniques have been proposed, e.g., [10,11]. In parametric approaches, fixed basis of transfer functions are weighted by non-linear functions of the time-varying parameter. The works [12, 13] claim that the critical step is how to select a priori the basis functions to describe the system dynamics. An improper selection causes a structural bias. LPV state space-model identification methods have been proposed in [14, 15]. They allow the estimation of low-order models but maintain the inconvenient of basis selection. On the other hand, nonparametric techniques have been proposed in [16–18]. They yield an alternative way to face the bias problem by obtaining nonparametric models directly from data. For instance, in [19, 20] kernel-based LPV state-space models are identified. Nevertheless, this method requires an appropriate choice of a kernel in order to provide a suitable model that explains the nonlinearity of the physical system.

In this chapter, two techniques are employed to estimate LPV models for a laboratory scale web winding machine, extending the results presented in [21]. First, a unique LPV model is estimated for the complete range of variation of the reel radius. This model is estimated by means of the Set Membership state-space method recently proposed in [22], where the matrix coefficients are described by a linear combination of basis functions. Relevant features of this method are that the obtained model is almost-optimal (in a worst-case sense) and sparse (i.e. the vector of linear combination coefficients has only a few non-zero elements). Then, a set of local LTI models are estimated applying Predictor-Based Subspace methods that allow us to handle closed-loop data, see [23]. Then, an LPV model is obtained as a weighted sum of local models employing radial basis functions with fixed centers. The weighting functions depend on the reel radius and the models are selected minimizing a quadratic criterion solving a convex optimization problem.

The chapter is organized as follows. First, Section 1.2 describes the Sparse Set Membership Identification method of state-stace LPV systems. Then, the interpolated identification of state-space LPV systems is described in Section 1.3. The experimental setup and a comparison of the results obtained with the two identification methods are presented in Section 1.4. Finally, the conclusions of the work are presented in Section 1.5.

1.2 Sparse Set Membership identification of state-space LPV systems

In this section, a variant of the Sparse Set Membership (SSM) approach proposed in [22] for state-space LPV system identification is described.

Consider a discrete-time LPV system in the following state-space observability form:

$$\begin{aligned} \mathbf{x}(k+1) &= \mathbf{A}(\mathbf{p}(k))\,\mathbf{x}(k)+\mathbf{B}(\mathbf{p}(k))\,\mathbf{u}(k)+\mathbf{B}_w w(k) \\ y(k) &= \mathbf{C}\mathbf{x}(k)+v(k) \end{aligned} \tag{1.1}$$

$$\begin{aligned} \mathbf{A}(\mathbf{p}(k)) &= \begin{bmatrix} 0 & 1 & \cdots & 0 \\ \vdots & \vdots & \ddots & \vdots \\ 0 & 0 & \cdots & 1 \\ f_{n_x}(\mathbf{p}(k)) & f_{n_x-1}(\mathbf{p}(k)) & \cdots & f_1(\mathbf{p}(k)) \end{bmatrix} \\ \mathbf{B}(\mathbf{p}(k)) &= \begin{bmatrix} f_{n_x+1}(\mathbf{p}(k)) & \cdots & f_{2n_x}(\mathbf{p}(k)) \end{bmatrix}^T \\ \mathbf{B}_w &= \begin{bmatrix} 0 & \cdots & 0 & 1 \end{bmatrix}^T \\ \mathbf{C} &= \begin{bmatrix} 1 & 0 & \cdots & 0 \end{bmatrix} \end{aligned}$$

where $\mathbf{x}(k) \in \mathbb{R}^{n_x}$ is the state, $\mathbf{u}(k) \in \mathbb{R}^{n_u}$ is the input, $y(k) \in \mathbb{R}$ is the output, $\mathbf{p}(k) \in P \subset \mathbb{R}^{n_p}$ is the time-varying parameter, P is a compact set, $w(k) \in \mathbb{R}$ accounts for all the process noises acting on the system, $v(k) \in \mathbb{R}$ is a measurement noise, $\mathbf{A}(\mathbf{p}(k))$, $\mathbf{B}(\mathbf{p}(k))$, $\mathbf{B}_w$ and $\mathbf{C}$ are matrices/vectors of suitable dimensions, and

$$f_i : \mathbb{R}^{n_p} \to \begin{cases} \mathbb{R}, & 1 \le i \le n_x, \\ \mathbb{R}^{1\times n_u}, & n_x < i \le 2n_x. \end{cases}$$

We consider here the multi-input-single-output (MISO) case for simplicity of notation. The generalization to the multi-input-multi-output (MIMO) case is straightforward, see [22].

Suppose that this system is not known, but a set of input-output data

$$DS = \{\mathbf{u}(k), y(k), \mathbf{p}(k)\}_{k=1-n_x}^{L} \tag{1.2}$$

is available. Then, assume that the noise

$$d(k) \doteq w(k-n_x) + v(k) - \sum_{i=1}^{n_x} f_i(\mathbf{p}(k-n_x))\, v(k-i), \tag{1.3}$$

accounting for both the noises $w(k)$ and $v(k)$, is unknown but bounded as

$$\|d\|_h \le \mu \tag{1.4}$$

where $\|\cdot\|_h$ is a vector ℓ_h norm.

In this section, the problem of identifying the system (1.1) from the data set (1.2) is considered. Note that bound (1.4) on the noise affecting the measurements of $y(t)$ does not assume any statistical property on $d(t)$, then the method presented here is valid for data generated in open-loop or in closed-loop.

Since system (1.1) is univocally defined by the vector-valued function $f = [f_1 \cdots f_n]^T$, $n \doteq (1+n_u)n_x$, its identification can be performed by finding an estimate $\widehat{f}$ of f giving a "small" identification error

$$E\left(f,\widehat{f}\right) \doteq \left\|\xi\left(f,\widehat{f}\right)\right\|_q \tag{1.5}$$

where

$$\xi\left(f,\widehat{f}\right) \doteq \left[\xi\left(f_1,\widehat{f}_1\right) \cdots \xi\left(f_n,\widehat{f}_n\right)\right]^T$$
$$\xi\left(f_i,\widehat{f}_i\right) \doteq \left\|f_i-\widehat{f}_i\right\|_s,$$

$\|\cdot\|_q$ is a vector ℓ_q norm and $\|\cdot\|_s$ is a functional L_s norm evaluated over the set $P \subset \mathbb{R}^{n_p}$.

An algorithm for deriving such an estimate is now presented. For simplicity, we consider here the case where the first $n_x - 1$ elements $f_{n_x+1},\ldots,f_{2n_x-1}$ of the matrix $B(p(k))$ are null. The general case can be treated in a similar way, at the expense of a more complicated notation. It can be noted that, even supposing null these $n_x - 1$ elements, the LPV model structure (1.1) is general enough to capture quite complex systems, as demonstrated in Section 1.4.1, where identification of a real web winding machine is carried out.

Let $BF \doteq \{\beta_j : \mathbb{R} \to \mathbb{R},\ j = 1,\ldots,m\}$ be a set of basis functions (guidelines for the choice of these functions are given in [22]). Define the following quantities:

$$\begin{aligned}
\mathbf{Y} &\doteq [y(1) \cdots y(L)]^T \\
\Lambda_i &\doteq \begin{bmatrix} \beta_1(\rho_i(1)) & \cdots & \beta_m(\rho_i(1)) \\ \vdots & \ddots & \vdots \\ \beta_1(\rho_i(L)) & \cdots & \beta_m(\rho_i(L)) \end{bmatrix} \in \mathbb{R}^{L\times m} \\
\Psi &\doteq \begin{bmatrix} \phi_1\Lambda_1 & \cdots & \phi_n\Lambda_n \end{bmatrix} \in \mathbb{R}^{L\times N}
\end{aligned} \tag{1.6}$$

where $i = 1,\ldots,n$, $N \doteq nm$,

$$\begin{aligned}
\rho_i(k) &\doteq \begin{cases} \mathbf{p}(k-n_x), & 1 \le i \le n_x \\ \mathbf{p}(k+n_x+1-i), & n_x < i \le n \end{cases} \\
\varphi(k) &\doteq [y(k-1) \cdots y(k-n_x) \cdots \\
&\qquad \mathbf{u}(k-1) \cdots \mathbf{u}(k-n_x)]^T \\
\phi_i &\doteq \mathrm{diag}([\varphi_i(1)\cdots\varphi_i(L)]),
\end{aligned} \tag{1.7}$$

and φ_i denotes the ith component of the regressor $\varphi(k)$. Note that, while the set BF consists of m functions, the total number of basis functions actually used for identification is $N \doteq nm$. Indeed, in the matrix Ψ, each function of BF is multiplied by each component of the regressor $\varphi(k)$, and the total number of regressor components is $n = (1+n_u)n_x$.

SSM algorithm

1. Solve the optimization problem

$$\begin{aligned} &\theta^1 = \arg\min_{\theta\in\mathbb{R}^N} \|\theta\|_1 \\ &\text{subject to} \quad \|\mathbf{Y} - \Psi\text{`}\theta\|_h \leq \mu. \end{aligned} \tag{1.8}$$

2. Consider the set of indices

$$\overline{\zeta}\left(\theta^1\right) \doteq \left\{i \in \{1,2,\ldots,N\} : \theta_i^1 = 0\right\}$$

where θ_i^1 are the components of the vector θ^1.
Obtain the coefficient vector θ^* as the solution of the following optimization problem:

$$\begin{aligned} &\theta^* = \arg\min_{\theta\in\mathbb{R}^N} \|\mathbf{Y} - \Psi\theta\|_h \\ &\text{subject to} \quad \theta_i = 0,\ i \in \overline{\zeta}\left(\theta^1\right). \end{aligned} \tag{1.9}$$

3. Define the coefficients $\alpha_{i,j}^* \doteq \theta_{(i-1)m+j}^*$. An estimate of the unknown function f is given by $f^* = [f_1^* \ \cdots \ f_n^*]^T$, where

$$f_i^*(\rho) = \sum_{j=1}^{m} \alpha_{i,j}^* \beta_j(\rho). \tag{1.10}$$

4. The resulting LPV model is a system of the form (1.1) with $f = f^*$. ■

Remark 1: *In [22] it is shown that, assuming a Lipschitz continuous* residue functions $\Delta_i \doteq f_i - f_i^*$, $i = 1,\ldots,n$, *the estimate* f^* *is almost-optimal (in a worst-case sense) for any* ℓ_q *and* ℓ_h *vector norms, and any* L_s *functional norm. That is,*

$$EW(f^*) \leq 2 \inf_{\widehat{f}} EW\left(\widehat{f}\right)$$

where EW is the worst-case identification error*, defined as*

$$EW\left(\widehat{f}\right) \doteq \sup_{g\in FFS} E\left(g, \widehat{f}\right)$$

and FFS is the Feasible Function Set*, i.e. the set of all functions consistent with prior assumptions and measured data. This shows that the worst-case identification error of* f^* *is at most twice the lowest achievable one. See [22] for more details and for a rigorous proof of this result.* ■

In the reminder of this section, the sparsity properties of the SSM algorithm and of the resulting estimate f^* are briefly discussed. A *sparse* function is a linear combination of many basis functions, where the vector of linear combination coefficients is sparse, i.e. it has only a few non-zero elements. The *sparsity* of a vector θ is typically measured by the ℓ_0 quasi-norm, defined as the number of its non-zero elements. Sparse identification can thus be performed by looking for a coefficient vector of the basis function linear combination with a small ℓ_0 quasi-norm. However, the ℓ_0 quasi-norm is a non-convex function and its minimization is in general an NP-hard problem. Two main approaches are commonly adopted to deal with this

issue: convex relaxation and greedy algorithms. In convex relaxation, a suitable convex function, e.g. the ℓ_1 norm, is minimized instead of the ℓ_0 quasi-norm [24–26]. Indeed, the ℓ_1 norm is the convex envelope of the ℓ_0 quasi-norm, and its minimization yields a sparse vector. In greedy algorithms, the sparse solution is obtained iteratively [27].

The above SSM algorithm is essentially an improved ℓ_1 algorithm: In step 1, an optimization problem is solved, where the ℓ_0 quasi-norm is replaced by the ℓ_1 norm. The vector θ^1 derived in step 1 is thus sparse and guarantees a bounded prediction error $\left\|\mathbf{Y}-\Psi\theta^1\right\|_h$. However, θ^1 is not ensured to give the minimum prediction error among all vectors with the same sparsity. Then, a vector θ^* is obtained in step 2, having the same sparsity of θ^1 and giving minimum prediction error. In [28], a condition is provided, under which θ^* is maximally sparse (i.e. with minimum ℓ_0 quasi-norm).

Note that the sparsity property is of high practical interest. Indeed, if θ^* is sparse, the evaluation of $f_i^*(\rho)$ is very "fast" and can be performed in on-line applications where "small" sampling periods are utilized (e.g. model predictive control, gain scheduling).

1.3 Interpolated identification of state-space LPV systems

A classic approach to the identification of systems of the form (1.1), is to perform local experiments guaranteeing constant values of the parameter $\mathbf{p}(k)=\bar{\mathbf{p}}\in\mathbb{R}$ and then to build an interpolated LPV model. The combination of local models to build a LPV system is not a trivial task. If common basis are employed in the local identification step, the structure proposed in [29] can be employed. When state-space models are estimated, similarity transformations that allow the combination of local models must be pursuit, see e.g. [30]. The complexity of the aforementioned methods stems from the fact that a common state vector is required for the local models to build the interpolation. To avoid this limitation, in this paper, the interpolated model is constructed as the sum (*parallel connection*) of local models.

For a given constant value $\bar{p}_i$, the system (1.1) can be expressed as

$$\begin{aligned}\mathbf{x}(k+1) &= \mathbf{A}(\bar{p}_i)\mathbf{x}(k)+\mathbf{B}(\bar{p}_i)\mathbf{u}(k)+\mathbf{B}_w w(k)\\ y_i(k) &= \mathbf{C}(\bar{p}_i)\mathbf{x}(k)+v(k)\end{aligned}$$

and thus it can be identified using standard estimation techniques for LTI systems. When it is not possible to maintain a constant parameter p during the experiment, but f_i are smooth functions of p, it can be assumed that the system dynamics remain almost constant when p belongs to an interval $[\underline{p},\overline{p}]$, where the width of the interval depends on the smoothness of the functions f_i.

The interpolated model generates an output formed by a weighted sum of the outputs predicted by the local models,

$$\hat{y}_{LPV}(k)=\sum_{i=1}^{l}\alpha_i\sigma_i(p(k))y_i(k), \tag{1.11}$$

where l is the number of local models, α_i is a fixed weigthing parameter and $\sigma_i(p(k))$ is an activation function of the time varying parameter $p(k)$.

The concept behind (1.11) is a gain-scheduling structure. The activation functions $\sigma_i(p(k))$ select as global output $\hat{y}_{LPV}(k)$, the output of the local system i, whose dynamcis behave as system (1.1) for the current parameter $p(k)$.

Given a set of input-output data

$$DS = \{\mathbf{u}(k), y(k), p(k)\}_{k=1-n_x}^{L},$$

the aim of the procedure presented here is to estimate several local LTI models for different intervals of the parameter $p(k)$, and then to combine them in order to construct an Interpolated LPV Model (ILM). The algorithm consists of two main parts, as shown in the following.

ILM algorithm

1) *Local model estimation algorithm*

- Group the samples in l identification data set as:

$$DS_i = \left\{\mathbf{u}(k), y(k), p(k) : \underline{p}_i \leq p(k) < \overline{p}_i\right\}, i = 1,2,...l.$$

  where l is the number of local models.
- Estimate an appropriate order of the local model for each data set DS_i and obtain the model matrices $\hat{\mathbf{A}}_i, \hat{\mathbf{B}}_i, \hat{\mathbf{C}}_i$ and noise variances $var(w)$ and $var(v)$. Note that different orders can be selected for local models as no state combination is performed in the interpolation. Diverse LTI identification methods can be employed to estimate local models. For example, when the system is operated in open-loop, robust subspace algorithms, such as `N4SID` [31], can be applied. When closed-loop data are employed, recursive identification techniques can be exploited [32, 33].
- Obtain the simulated output $\hat{y}_i(k)$ for the estimated model as:

$$\hat{y}_i(k) = \sum_{r=0}^{k-1} \hat{\mathbf{C}}_i \hat{\mathbf{A}}_i^{k-r-1} \hat{\mathbf{B}}_i u(r),\ k = 1, \ldots, L.$$

2) *Interpolation function estimation*

- Compute the vector $\alpha = [\alpha_1 \ \cdots \ \alpha_l]^T$ by means of the following quadratic optimization problem:

$$\begin{array}{rcl} \alpha^* & = & \arg\min_{\alpha \in \mathbb{R}^l} \left\| \mathbf{Y} - \hat{\mathbf{Y}}_{LPV} \right\|_2 \\ & & \text{subject to } \ 0 \leq \alpha_i \leq 1. \end{array}$$

  where $\hat{\mathbf{Y}}_{LPV} \doteq [\hat{y}_{LPV}(1) \ \cdots \ \hat{y}_{LPV}(L)]^T$ and

$$\hat{y}_{LPV}(k) = \sum_{i=1}^{l} \alpha_i \sigma_i(p(k)) \hat{y}_i(k)$$

  with

$$\sigma_i(p) = e^{-\beta_i (p - p_i^c)^2}$$

where $p_i^c = 0.5(\underline{p}_i + \overline{p}_i)$ and β_i is a fixed parameter. Radial basis functions with Gaussian form are selected to interpolate the models output, however any radial basis set can be employed.

- The LPV model is built as a weighted sum of the local models output:

$$\hat{y}_{LPV}(k) = \sum_{r=1}^{l} \alpha_i^* \sigma_i(p(k)) \hat{y}_i(k).$$

■

Remark 2: *The order of the complete system is*

$$n_{ILM} = \sum_{r=1}^{l} n_r.$$

That is, the sum of the orders (state dimension) of the local LTI models. ■

1.4 Web Winding System Identification

1.4.1 The Web Winding System

The considered web winding system is a laboratory scale plant (see Fig. 1.1), where it is required to transport material at a desired tension and speed, ensuring that the web (in this case magnetic tape) is not broken or deteriorated. This system includes the following components:

- Two DC motors with optical encoder (and with angular speeds ω_1, ω_2) drive the material, each one connected to a reel.
- An optical encoder coupled to one of the pulleys that guides the web measures the web transport speed (angular speed ω_3),
- A dancer arm system measures the web tension. Its rotation axis is connected to a linear potentiometer.
- A radius meter for one of the reels (the radius is denoted by r_2).

Fig. 1.2 shows a scheme of the plant operation when the web is rolled around the reel connected to motor 2. The difference between tensions T_1 and T_2 causes the transport of the material with a web speed ω_3 and a variation of the height h.

The voltages applied to motors 1 (V_1) and 2 (V_2) are the system input, the material transport speed (ω_3) is the output of interest, the radius r_2 is the time-varying parameter.

Assuming that the motors 1 and 2 have equal electromechanical characteristics, that the slip between the tape and bearings is negligible, that the dancer arm moves vertically only, and that all the fixed axes of the plant have null moment of inertia,

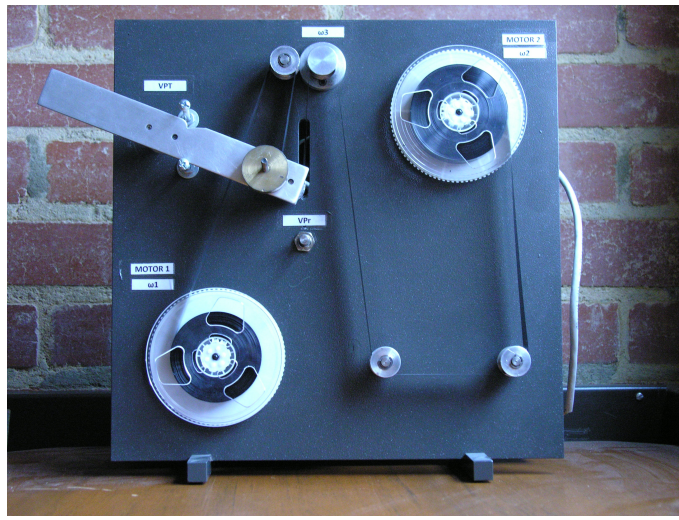

Figure 1.1 A picture of the web winding system

the system dynamics can be described by the following set of equations:

$$J_i(t)\dot{\omega}_i(t) = -B_i\omega_i(t) + \frac{k_T}{R_a}(V_i(t) - k_V\omega_i(t)) + r_i(t)T_i(t);\ \ i = 1,2 \tag{1.12}$$

$$\dot{r}_i(t) = \frac{s}{2\pi}\omega_i(t);\ \ i = 1,2 \tag{1.13}$$

$$\dot{\omega}_3(t) = \frac{r_3}{J_3}(T_2(t) - T_1(t)) \tag{1.14}$$

$$\dot{T}_1(t) = k_E(r_3\omega_3(t) - r_1(t)\omega_1(t)) + D(r_3\dot{\omega}_3(t) - r_1(t)\dot{\omega}_1(t) - \dot{r}_1(t)\omega_1(t)) \tag{1.15}$$

$$\dot{T}_2(t) = k_E(r_2(t)\omega_2(t) - r_3\omega_3(t)) + D(r_2(t)\dot{\omega}_2(t) + \dot{r}_2(t)\omega_2(t) - r_3(t)\dot{\omega}_3(t)) \tag{1.16}$$

where ω_i are the motors speed, J_i are the time-varying moments of inertia of each motor axis, r_i are time-varying radius of the motor loads. The model constant param-

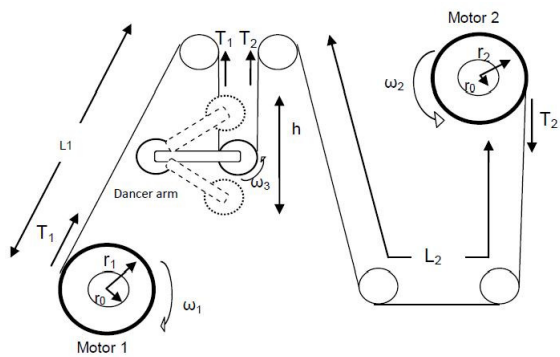

Figure 1.2 A scheme of the web winding system

eters are the following: B_i are the axis friction coefficients, k_T is the motor torque constant, k_V is the motor voltage constant, R_a is the armature resistance, s is the tape thickness, r_3 is the dancer arm radius, J_3 is the dancer arm moment of inertia, k_E is the tape elastic constant, D is the tape damping constant.

From (1.12)-(1.16), it can be seen that the web winding system is a quite complex plant, approximately described by a set of 7 non-linear and time-varying differential equations. Moreover, the web winding system, by nature, is input-output unstable [1–4]. Due to these features, linear control systems do not give in general adequate performances in terms of disturbance rejection. On the contrary, gain-scheduling controllers are expected to provide high performances, since these controllers can effectively deal with nonlinearities and time-varying parameters. This motivates the need of accurate LPV models, which can be used to design efficient gain-scheduling controllers. Note that obtaining an LPV model from equations (1.12)-(1.16) is not practicable, since these equations involve several uncertain parameters, which are in general difficult to measure or estimate. Note also that, because of the intrinsic instability of the system, model identification and validation are in general quite difficult tasks.

1.4.2 Experiment Description

The web winding system previously described is input-output unstable in open loop, therefore the identification experiments have been performed in closed-loop. Two decoupled PID controllers have been used to regulate the web transport speed ω_3 and web tension T_1 by controlling the dancer arm position θ, see fig. 1.3. These controllers have been tuned experimentally in order to stabilize the plant in the complete operation range.

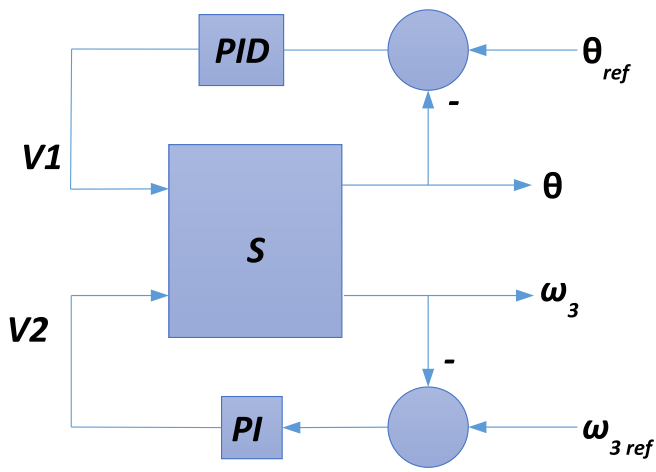

Figure 1.3 Control system employed for generating the data sets.

For the system identification process, the signals V_1, V_2 and ω_3 were recorded with a sample time of 40 ms. It has been observed that the system bandwidth does

not exceed 10 Hz. Each experiment started with no material on the reel attached to motor 2 and finished when it reached its maximum capacity. The duration of each experiment was about 90 seconds (2250 samples).

The input signals for each experiment is formed by a sequence of set-point commands for the two PID loops. Five experiments have been carried out, where different set-point signals have been used:

- Pseudorandom binary sequence (PRBS). This signal has a peak amplitude of 3.5 degrees around the set-point for the dancer arm control loop and 21 rad/s for the web speed control loop. Two experiments, called PRBS1 and PRBS2, have been performed using a PRBS input signal generated as a 4095-steps random sequence, the only difference between these two experiments is the realization of measurement noise and uncontrollable disturbances.
- Random binary sequence (RBS). This signal has a peak amplitude of 5 degrees around the set-point for the dancer arm control loop and 20 rad/s for the web speed control loop. The switching time is 10 sample instants, with switching probability 0.2.
- Sum of sinusoids (SINE). This signal is formed by 20 sinusoids and has a maximum amplitude of 8 degrees to the dancer arm control loop and 48 rad/s to the speed control loop.
- Random Gaussian sequence (RGS): This signal has a peak amplitude of 10 degrees around the set-point for the dancer arm control loop and 40 rad/s for the web speed control loop. It is generated as a white Gaussian sequence filtered by a low-pass filter with cut-off frequency 1 Hz.

The data set has been partitioned as follows:

- *Estimation data set*: Data generated in the PRBS1 and RBS experiments.
- *Validation data set*: Data generated in all the five experiments.

1.4.3 Sparse Set Membership LPV model

Identification of the web winding system has been performed by means of the Sparse Set Membership (SSM) approach summarized in Section 1.2. The optimization problems in the SSM algorithm have been solved using the CVX package [34].

The following set of $m = 8$ basis functions has been used:

$$BF \doteq \{1, \rho, \rho^2, \rho^3, \rho^4, \rho^{-1}, \rho^{-2}, \rho^{-3}\}.$$

Model orders n_x in the range $[1, 15]$ have been considered. For each order, a model has been identified on the estimation data set by means of the SSM algorithm. The value of μ has been taken slightly larger than the minimum value for which the optimization problem (1.8) was feasible (see [22] for more details). The chosen values of μ resulted to range in the interval $[30, 40]$.

The identified models have been compared in simulation on the estimation data set, and the one with order $n_x = 13$ provided the best results. Note that, while the set BF consists of $m = 8$ functions, the total number of basis functions actually used for the identification of this model is $N \doteq nm = (1 + n_u)n_x m = 312$. Indeed, each

function of BF has been multiplied by each regressor to build the matrix Ψ in (1.6), and the total number of regressors is $n = (1+n_u)n_x = 39$. Among these 312 basis functions, the SSM algorithm selected 37 functions. A model of order $n_x = 13$, has thus been chosen and called SSM.

1.4.4 Interpolated LPV model

Identification of the web winding system has been performed by means of the interpolation-based approach described in Section 1.3. In the case of the web winding machine, it is not possible to maintain a constant reel radius, but it is known that the web moves always from motor 1 to motor 2, then r_1 and r_2 are monotonically decreasing and increasing functions of time, respectively.

The estimation set DS has been split into l subsets DS_i. Each one containing input and output data corresponding to a radius interval $r_2 \in [\underline{p}_i, \overline{p}_i]$, forming equally spaced intervals of the reel radius range. The ILM algorithm has been applied for several amounts of subsystems in the range $[2,\ldots,15]$. Note that for $l = 15$, each local data set has 150 samples on average.

The Predictor-Based Subspace Identification Toolbox [35] has been employed for local models estimation. For each data set DS_i, an order 4 has been suggested by the Predictor-Based Subspace Identification Toolbox. For the construction of the weighting functions, the value of β has been adjusted according to the number of local models. Centers p_i^c of the radial basis functions have been set to the interval centers $(\underline{p}_i + \overline{p}_i)/2$. The QP problem has been solved using the CVX package [34].

The identified models have been compared in simulation on the estimation data set, and the one with $l = 3$ sub-models provided the best results. Then, an interpolated model of order $n_{ILM} = 12$ has been selected and called ILM.

Finally, a single LTI model has been identified from the estimation set employing the Predictor-Based Subspace Identification Toolbox [35]. Several orders have been tried and the model that showed better performance on the estimation set was a model with $n = 6$. Thsi model is named LTI in the following.

1.4.5 Model validation and results

The three models identified in the previous subsections have been simulated in open-loop using as inputs the measured voltages on the validation data sets. Then, the outputs provided by the models have been compared to the measured output signals. The FIT index and the relative maximum error (RM) have been used to evaluate the model quality. These indexes have been computed as

$$FIT = 100\left(1 - \frac{\left\|\widetilde{\mathbf{Y}} - \mathbf{Y}_s\right\|_2}{\left\|\widetilde{\mathbf{Y}} - \text{mean}(\widetilde{\mathbf{Y}})\right\|_2}\right) \tag{1.17}$$

$$RM = 100\frac{\left\|\widetilde{\mathbf{Y}} - \mathbf{Y}_s\right\|_\infty}{\left\|\widetilde{\mathbf{Y}} - \text{mean}(\widetilde{\mathbf{Y}})\right\|_\infty} \tag{1.18}$$

where $\widetilde{\mathbf{Y}} = [y(1) \ldots y(L_e)]^T$ and $\mathbf{Y}_s = [y_s(1) \ldots y_s(L_e)]^T$ are the measured and simulated output signals, respectively, and L_e is the experiment length.

The obtained results are shown in Tables 1.1 and 1.2 for all the five experiments in the validation set. A comparison between the measured and simulated outputs is shown in Figs. 1.4, 1.5, 1.6 and 1.7 for four experiments of the validation set. From these tables and figures, it can be seen that both the LPV models are able to explain quite accurately data not employed for identification.

Note that the ILM model is formed by three LTI models of the third order, yielding an overall model of order 12, whereas the SSM model is of order 13. It is important to remark that some of the 37 basis functions selected by the SSM algorithm during the identification of the SSM model involve regressors of order 12 and 13, confirming that such orders are necessary to obtain accurate results.

Model	PRBS1	PRBS2	RBS1	SINE1	RGS1
SSM	95	93	92	90	90
ILM	86	85	89	83	90
LTI	86	85	89	83	90

Table 1.1 Model FIT indexes on the validation data set.

Model	PRBS1	PRBS2	RBS1	SINE1	RGS1
SSM	5	5	6	8	6
ILM	15	15	18	17	8
LTI	86	85	89	83	90

Table 1.2 Model RM errors on the validation data set.

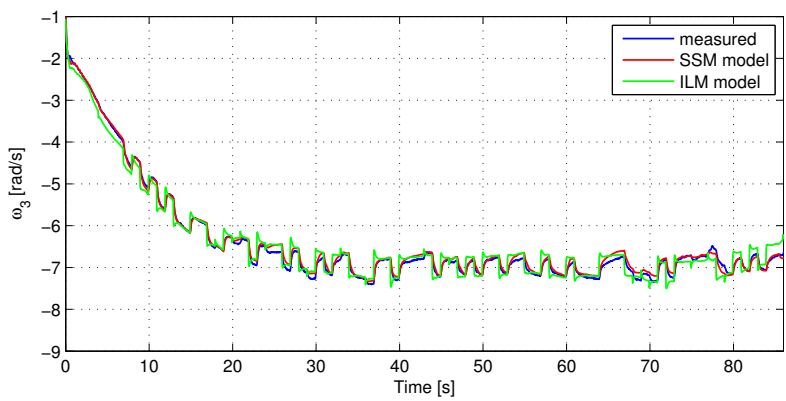

Figure 1.4 Experiment PRBS2: comparison between measured and simulated outputs.

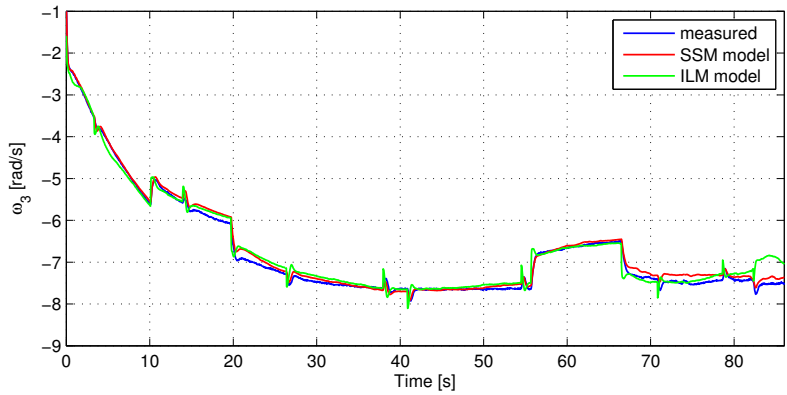

Figure 1.5 Experiment RBS1: comparison between measured and simulated outputs.

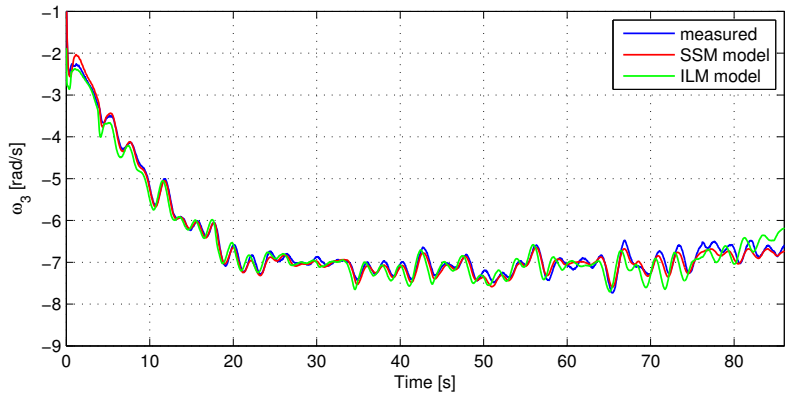

Figure 1.6 Experiment SINE1: comparison between measured and simulated outputs.

1.5 Conclusion

Two methods for the identification of LPV models have been applied to a laboratory scale web winding machine, describing the web speed dynamics and employing the reel radius as the time-varying parameter. A unique LPV model in state-space form has been estimated, where the matrix coefficients are described by a linear combination of basis functions. The coefficients of the basis expansion have been selected in order to maximize the model sparsity and to guarantee at the same time its almost-optimality (in a Set Membership framework). A second model was constructed as an interpolation of local LTI models, estimated by sub-space methods. Three time-invariant models have been identified for equally spaced reel radius intervals and a weighted sum of the LTI models outputs has been formed minimizing a quadratic criterion. Both the models are able to explain fresh data, not used in the identifica-

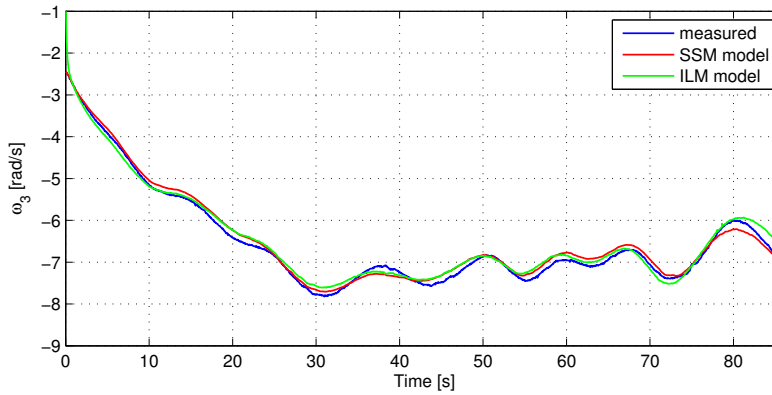

Figure 1.7 Experiment RGS1: comparison between measured and simulated outputs.

tion phase. Better results have been obtained with the unique LPV model in terms of FIT coefficient and maximum error, while the interpolated model required a simpler identification process.

References

[1] Liu Z. Dynamic analysis of center-driven web winder controls. In: Industry Applications Conference, 1999. Thirty-Fourth IAS Annual Meeting. Conference Record of the 1999 IEEE. vol. 2. IEEE; 1999. p. 1388–1396.

[2] Benlatreche A, Knittel D, Ostertag E. Robust decentralised control strategies for large-scale web handling systems. Control Engineering Practice. 2008;16(6):736–750.

[3] Lynch AF, Bortoff SA. Nonlinear tension observers for web machines. Automatica. 2004;40(9):1517–1524.

[4] Chen CL, Chang KM, Chang CM. Modeling and control of a web-fed machine. Applied Mathematical Modelling. 2004;28(10):863–876.

[5] Noura H, Bastogne T. Tension optimal control of a multivariable winding process. In: American Control Conference, 1997. Proceedings of the 1997. vol. 4. IEEE; 1997. p. 2499–2503.

[6] Bastogne T, Noura H, Sibille P, et al. Multivariable identification of a winding process by subspace methods for tension control. Control Engineering Practice. 1998;6(9):1077–1088.

[7] Garnier H, Gilson M, Young P, et al. An optimal IV technique for identifying continuous-time transfer function model of multiple input systems. Control engineering practice. 2007;15(4):471–486.

[8] Xu Y, Wang D, Zhang Q. Modeling and Robust Control of Web Winding System with Sinusoidal Tension Disturbance. In: Mechatronics and Automa-

tion, Proceedings of the 2006 IEEE International Conference on. IEEE; 2006. p. 1958–1963.

[9] Xu Y. Modeling and LPV control of web winding system with sinusoidal tension disturbance. In: Control and Decision Conference, 2009. CCDC'09. Chinese. IEEE; 2009. p. 3815–3820.

[10] Tóth R. Modeling and identification of linear parameter-varying systems. Netherlands: Springer; 2010.

[11] dos Santos PL. Linear Parameter-Varying System Identification: New Developments and Trends. Advanced series in electrical and computer engineering. World Scientific Publishing Company; 2012. Available from: https://books.google.com.co/books?id=4AjU84zbhiMC.

[12] van Wingerden JW, Verhaegen M. Subspace identification of multivariable LPV systems: A novel approach. Proceedings of the 2008 IEEE International Symposium on Computer-Aided Control System Design. 2008;2:840–845.

[13] Toth R, Abbas HS, Werner H. On the state-space realization of lpv input-output models: Practical approaches. IEEE Transactions on Control Systems Technology. 2012;20(1):139–153.

[14] Larimore WE, Cox PB, Toth R. CVA identification of nonlinear systems with LPV state-space models of affine dependence. Proceedings of the American Control Conference. 2015;2015-July(1):831–837.

[15] Tanelli M, Ardagna D, Lovera M. Identification of LPV state space models for autonomic web service systems. IEEE Transactions on Control Systems Technology. 2011;19(1):93–103.

[16] Hsu K, Vincent TL, Poolla K. Nonparametric methods for the identification of linear parameter varying systems. Proc of the Int Symposium on Computer-Aided Control System Design. 2008;(1):846–851.

[17] Goos J, Pintelon R. Continuous time frequency domain LPV state space identification via periodic time-varying input-output modeling. Conference on Decision and Control. 2014;(5):2567–2572.

[18] Rizvi SZ, Mohammadpour J, Roland T. An IV-SVM-based Approach for Identification of State-Space LPV Models under Generic Noise Conditions. Conference on Decision and Control. 2015;(Cdc):7380–7385.

[19] Proimadis I, Bijil H, Van Wingerden JW. A kernel based approach for LPV subspace identification. IFAC Proceedings Volumes (IFAC-PapersOnline). 2015;p. 97–102.

[20] Rizvi SZ, Mohammadpour J, Tóth R. A kernel-based approach to MIMO LPV state-space identification and application to a nonlinear process syste,. IFAC Proceedings Volumes (IFAC-PapersOnline). 2015;p. 85–90.

[21] Ruiz F, Vuelvas J, Novara C. LPV model identification for a web winding system. IFAC Proceedings Volumes (IFAC-PapersOnline). 2012;16(part I):1779–1784.

[22] Novara C. Set membership identification of state-space LPV systems. In: dos Santos PL, Perdicoúlis TPA, Novara C, et al., editors. Linear Parameter-Varying System Identification – New Developments and Trends, Advanced

Series in Electrical and Computer Engineering Vol. 14. World Scientific; 2011. p. 65–93.

[23] Houtzager I, van Wingerden JW, Verhaegen M. VARMAX-based closed-loop subspace model identification. In: Decision and Control, 2009 held jointly with the 2009 28th Chinese Control Conference. CDC/CCC 2009. Proceedings of the 48th IEEE Conference on; 2009. p. 3370–3375.

[24] Fuchs JJ. Recovery of exact sparse representations in the presence of bounded noise. Information Theory, IEEE Transactions on. 2005 oct;51(10):3601 – 3608.

[25] Tropp JA. Just relax: convex programming methods for identifying sparse signals in noise. Information Theory, IEEE Transactions on. 2006 mar;52(3):1030 –1051.

[26] Donoho DL, Elad M, Temlyakov VN. Stable recovery of sparse overcomplete representations in the presence of noise. Information Theory, IEEE Transactions on. 2006 jan;52(1):6 – 18.

[27] Tropp JA. Greed is good: algorithmic results for sparse approximation. Information Theory, IEEE Transactions on. 2004 oct;50(10):2231 – 2242.

[28] Novara C. Sparse identification of nonlinear functions and parametric Set Membership optimality analysis. In: American Control Conference. San Francisco, USA; 2011. .

[29] Tóth R, Heuberger P, Van den Hof P. Asymptotically optimal orthonormal basis functions for LPV system identification. Automatica. 2009;45(6):1359–1370.

[30] De Caigny J, Camino JF, Swevers J. Interpolation-Based Modeling of MIMO LPV Systems. Control Systems Technology, IEEE Transactions on. 2011;19(1):46 –63.

[31] Overchee V, De Moor B. Subspace Identification for Linear Systems. Dordrecht, Holanda: Kluwer Academic Publishers; 1996.

[32] Chiuso A, Picci G. Consistency Analysis of Certain Closed-Loop Subspace Identification Methods. Automatica, Special Issue on System Identification. 2005;41(3):377–391.

[33] Houtzager I, van Wingerden JW, Verhaegen M. Fast-array Recursive Closed-loop Subspace Model Identification. In: Proceedings of the 15th IFAC conference on system identification (SYSID 2009). Saint Malo, France; 2009. .

[34] Grant M, Boyd S. CVX: Matlab Software for Disciplined Convex Programming, version 1.21; 2010. http://cvxr.com/cvx.

[35] Houtzager I, Gebraad PMO, van Wingerden JW, et al.. Predictor-based Subspace Identification Toolbox Version 0.5; 2012. http://www.dcsc.tudelft.nl/~datadriven/pbsid/.